Optical properties of the retroreflective array in spectroscopic instrumentation

Konan Peck and Michael D. Morris

Department of Chemistry, University of Michigan, Ann Arbor, Michigan 48109

(Received 20 August 1986; accepted for publication 24 October 1986)

The distribution of retroreflected light from an array of corner cube prisms is measured as a function of angle of incidence and beam collimation. The imaging properties of the array are compared to those of a plane mirror in the presence and absence of phase perturbations. The implications for the use of a retroreflective array in absorbance measuring instrumentation are discussed.

INTRODUCTION

A retroreflective array (RRA) is an assembly of identical corner cube prisms arranged at uniform spacings, with their apertures forming a plane. The RRA behaves as an approximate phase conjugator,[1,2] which can compensate for many classes of aberrations in an optical system. As a purely passive system it operates equally well with coherent and incoherent light sources. In operation, the RRA breaks a beam of light into subbeams, each of which is subjected to retroreflection. If the array element density is high enough, the refractive index of the section of the medium sampled by each element will be nearly constant. In this case, the RRA performs a piecewise approximation to phase conjugation. Because the RRA is composed of passive reflectors only, it operates at the speed of light.

The RRA is one of several related systems,[3] which are all arrays of passive reflectors or refractors. Arrays of discrete corner cube prisms, or replicated arrays of corner cubes, are more readily constructed than most other approximate phase conjugators.

Although the unique advantage of the RRA is its application to incoherent sources, the first applications were as total reflectors in laser resonators. Divergence reductions of a factor of 4–10 have been observed in Nd glass,[4] CO_2,[5] iodine,[6] and dye lasers.[5,7] For this application coarse reflectors, including bicycle reflectors[5] and assemblies of 1-mm or larger aperture corner cubes,[4,6,7] have been used.

Approximate phase conjugation is only now emerging as a useful technique for the correction of refractive artifacts in absorbance measurements. Initial experiments using a retroreflective array (RRA) in a liquid chromatography absorbance detector showed a 4–6× improvement in signal/noise ratio relative to a conventional design.[8] In a recent application of the RRA to flame atomic absorption measurements,[9] we have observed about a sevenfold decrease in signal fluctuations resulting from local variations in flame refractive index. That work also demonstrated that the RRA has no effect on absorbance changes due to concentration perturbations, as expected.

These promising initial results suggest that retroreflective arrays may be useful in many absorbance measurement systems. Refractive artifacts are troublesome whenever high-precision or low-absorbance measurements are needed. If the system under study is inhomogeneous, is not isothermal, or is in motion during the measurement, refractive index gradients can perturb the measurement.

In both spectroscopic applications,[8,9] the RRA employed was an inexpensive plastic replica device, with coarse element spacing and unknown optical quality. The same or similar devices have been used in most investigations of the approximate phase conjugation properties of retroreflective arrays.[1,2] Crude arrays have been used because optical quality systems are not commercially available. If apertures below 1 mm are needed, a simple prism assembly is impractical. A small aperture RRA can be fabricated by the same techniques used to make diffraction gratings. However, the cost of fabricating a single example is prohibitively high for exploratory work.

The retroreflective array is not an ideal phase conjugator. The rational specification of optical quality arrays for spectroscopic instrumentation requires some knowledge of the optics of the arrays. Therefore, we have studied the properties of a retroreflective array in an optical system designed to test its limitations and identify the artifacts which it might introduce into spectroscopic measurements.

I. PROPERTIES OF THE RETROREFLECTIVE ARRAY

Because the array consists entirely of passive reflectors, it has no effect on light intensity except for losses at the reflective surfaces. The phase conjugation configuration does function as a double-pass optical system, doubling the sample absorbance. However, because of the presence of the beam splitter, this absorbance increase is offset by a decreased light flux at the detector. Ideally, there is no change in the shot-noise limited performance of the system relative to a single-pass measurement through a sample cell of the same length.

If the beam splitter passes fraction f of the incident light and reflects fraction $1-f$, then the light intensity at the detector is a factor of $f(1-f)$ lower than the intensity in a single-pass optical system. Therefore, the shot noise in the phase conjugation system will increase by the factor $1/\sqrt{f(1-f)}$. The maximum signal intensity reaches the detector if the array is lossless and an ideal 50:50 beam splitter is used. In this case, the intensity at the detector at low absorbance is 25% of the intensity in a single-pass system. The

 0034-6748/87/020189-08$01.30

signal/noise ratio increase from a doubled absorbance exactly balances the increase in shot noise. For an array with finite losses, or any beam splitter except a 50:50 device, the shot-noise limited minimum measurable absorbance will be higher than in a single-pass system.

Because individual rays are displaced by successive reflections, a retroreflective array inverts each component about the apex of the corner cube which reflects it. This local inversion is an inherent limitation to its applications in phase conjugation. A retroreflected wave encounters slightly different distortions from those which perturbed the wave in the forward direction. The retroreflective array can approximate a phase conjugator only for apertures sufficiently small that $dn/dx \simeq 0$ across them. The smaller the apertures of the individual retroreflectors the better the array can perform a phase aberration correction. However, this conclusion holds only when diffraction is negligible.

Unlike a true phase conjugator, the RRA returns a beam which does not converge exactly back to its source. The magnitude of the error depends upon the aperture size of the corner cube reflectors. The image rendered by a RRA will appear to be slightly fuzzy, even when in focus. The three phenomena which contribute to this effect are local inversion by the corner cubes, geometric spreading, and diffractive spreading.

If the aperture d is large, compared to the wavelength of light, geometric spreading[2] can limit the convergence, as shown in Fig. 1 for the two-dimensional limiting case. The divergence angle θ is given approximately by $\theta \simeq d/L$, where L is the array to source distance. This effect is wavelength independent.

In addition, diffractive spreading at the aperture causes a spreading of $\theta \simeq \lambda/d$, where λ is the wavelength of the incident light. Diffractive spreading becomes increasingly important at long wavelengths or small aperture.

Whether diffractive or geometric spreading is dominant depends on the relative magnitudes of d, L, and λ. Reflexite,

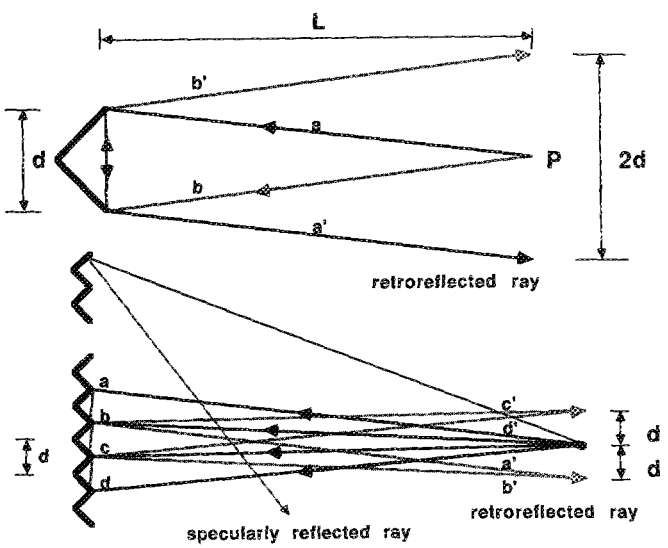

FIG. 1. Origin or geometric beam divergence in retroreflective array. L, distance from origin p to array surface; and d, effective aperture dimension. Upper diagram, single retroreflector; lower diagram, multielement array. Specular reflection at oblique angles of incidence is shown in lower diagram.

the material used in many previous experiments,[1,2,8,9] has $d \simeq 0.15$ mm. Taking the source to array distance to be 100 mm, the geometric spreading is 1.5 mrad. In practice, the source–array distance will be as great as 1000 mm. Therefore, 0.15–1.5 mrad is the range of geometric spreading expected. At the He–Ne red wavelength, 633 nm, the diffractive spreading is about 4 mrad. In the blue or ultraviolet, diffractive spreading is 2–3 times smaller. In an analytical instrument diffractive effects should be dominant with any array with 0.05–0.2-mm apertures.

Several effects contribute to the presence of reflected light at angles other than retroreflection. As shown in Fig. 1, a light ray striking an array surface at an oblique angle and near the aperture does not hit the other surfaces. It is reflected only once and appears at an angle far from retroreflection. There will be six such reflections in the array. A reflection is generated at each surface of the trihedral retroreflectors. There are two retroreflector orientations in the array. The beams will be directed at angles far from retroreflection. A similar effect contributes components from two surface reflections, with an oblique angle to the third surface.

The return beams from the individual elements of the array overlap. The overlap leads to interference,[1,10,11] as in other periodic structures, such as diffraction gratings. The retroreflected light will be distributed in orders. The first order is retroreflection. There will be a zero order, which will behave as specular reflection from the normal to the plane of the array. Generally, the interference is treated as one dimensional (linear), with a rectangular aperture function. Using these assumptions, Eq. (1) applies[11]:

$$\frac{I_\theta}{I_i} = \frac{1}{(2N+1)^2}\left(\frac{\sin[(2\pi a/\lambda)(\theta-\theta_i)]}{(2\pi a/\lambda)(\theta-\theta_i)}\right)^2 \times \left(\frac{\sin[(2\pi a)/\lambda)(2N+1)(\theta+\theta_i)]}{\sin[(2\pi a/\lambda)(\theta+\theta_i)]}\right)^2. \quad (1)$$

In Eq. (1), θ is the angle of the retroreflected light, relative to the grating normal, θ_i is the angle of incidence of the beam whose intensity is I_i at wavelength λ. The intensity of the retroreflected light is I_θ. The number of retroreflectors along a given direction is N and their size is $2a$. In general, theoretical treatments of diffractive effects predict that retroreflection ($\theta = \theta_i$) should contain most of the light.

Finally, if the array is formed in the rear surface of a material, Fresnel reflection from the planar front surface will be present. When present, this effect depends only on the refractive index of the array material.

II. EXPERIMENTAL

Most experiments were conducted with the apparatus shown in Fig. 2(a). A 1-mW He–Ne laser (Uniphase 1103P) was used as the light source. The He–Ne laser light was passed through a 10× collimating beam expander and microscope slide beam splitter to illuminate a retroreflective array (Reflexite, Reflexite Corp.). The retroreflective array was glued to a disk of aluminum mounted in a gimbal mirror mount. The returned light was reflected by the same beam splitter and focused by a 100-mm focal-length lens onto a photodiode apertured with a 1.5-mm-diam iris. The photo-

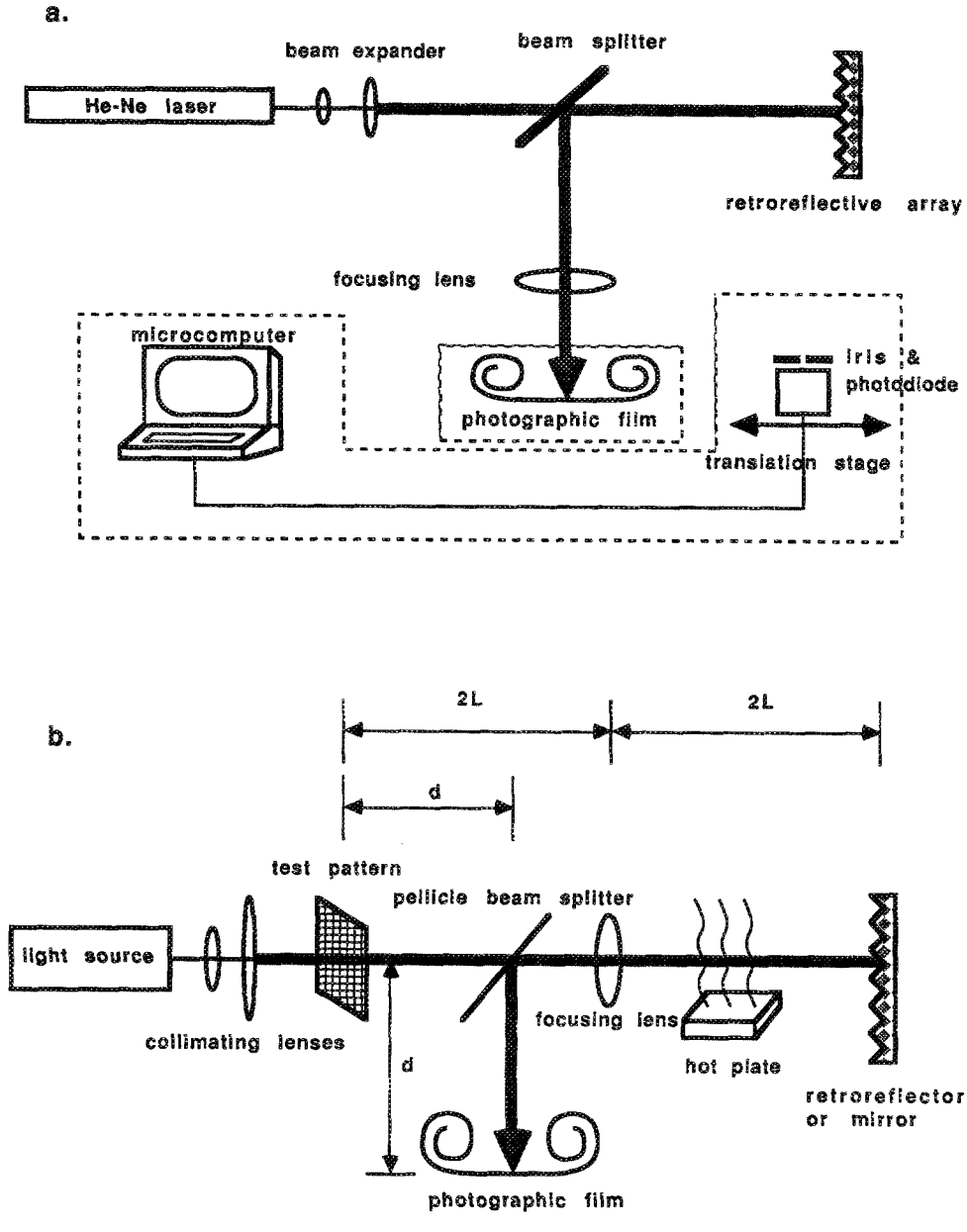

FIG. 2. (a) Experimental apparatus for measurement of angular dependence of retroreflective array properties. Photographic recording or digital storage of photodiode currents used, as described in text. (b) Apparatus for measurement of imaging properties of retroreflective array. Collimating lenses, fl. 50 and 500 mm; focusing lens, fl. $= L = 200$ mm; d, test pattern to beam splitter distance.

diode was mounted on a translation stage and scanned across the focused laser beam. The stage was driven by a motor/shaft encoder assembly which allowed measurement of its position with a resolution of 1 μ. For photographic records, the returned laser beam was focused directly onto photographic film mounted in a conventional single-lens reflex camera body.

The apparatus was modified, as in Fig. 2(b), for visual comparison of the imaging properties of the retroreflector with those of a plane mirror. A standard test pattern (Rolyn Optics, 705085) was placed in the light path. Collimated light, from either the He–Ne laser or a slide projector (Eastman Kodak) was used. A 5-μm-thick pellicle beam splitter with 33%/67% R/T coating was used to minimize ghost images. A 200-mm focal-length achromatic lens was used to focus the reflected image onto photographic film. The test pattern was located two focal lengths before the focusing lens, and the array or mirror was located two focal lengths after the lens. To introduce a phase perturbation, a 700-W hot plate was placed below the light path between the beam splitter and the reflector.

III. RESULTS AND DISCUSSION

Microscopic examination of Reflexite shows that the array element structure and spacing are quite uniform. This material should serve adequately to test the basic properties of any corner cube array. It is unlikely that the manufacturing tolerances are tight enough to allow a stamped plastic replica to behave as a coherent array. In addition, numerous small holes and cracks are visible in the aluminum coating. These defects degrade the overall performance of the array somewhat.

Figure 3 shows a series of diffraction patterns obtained with collimated laser light incident at different angles. The overall pattern is quite complex, because it is the resultant of several contributions. These include diffraction from the circular laser aperture, the individual triangular apertures of

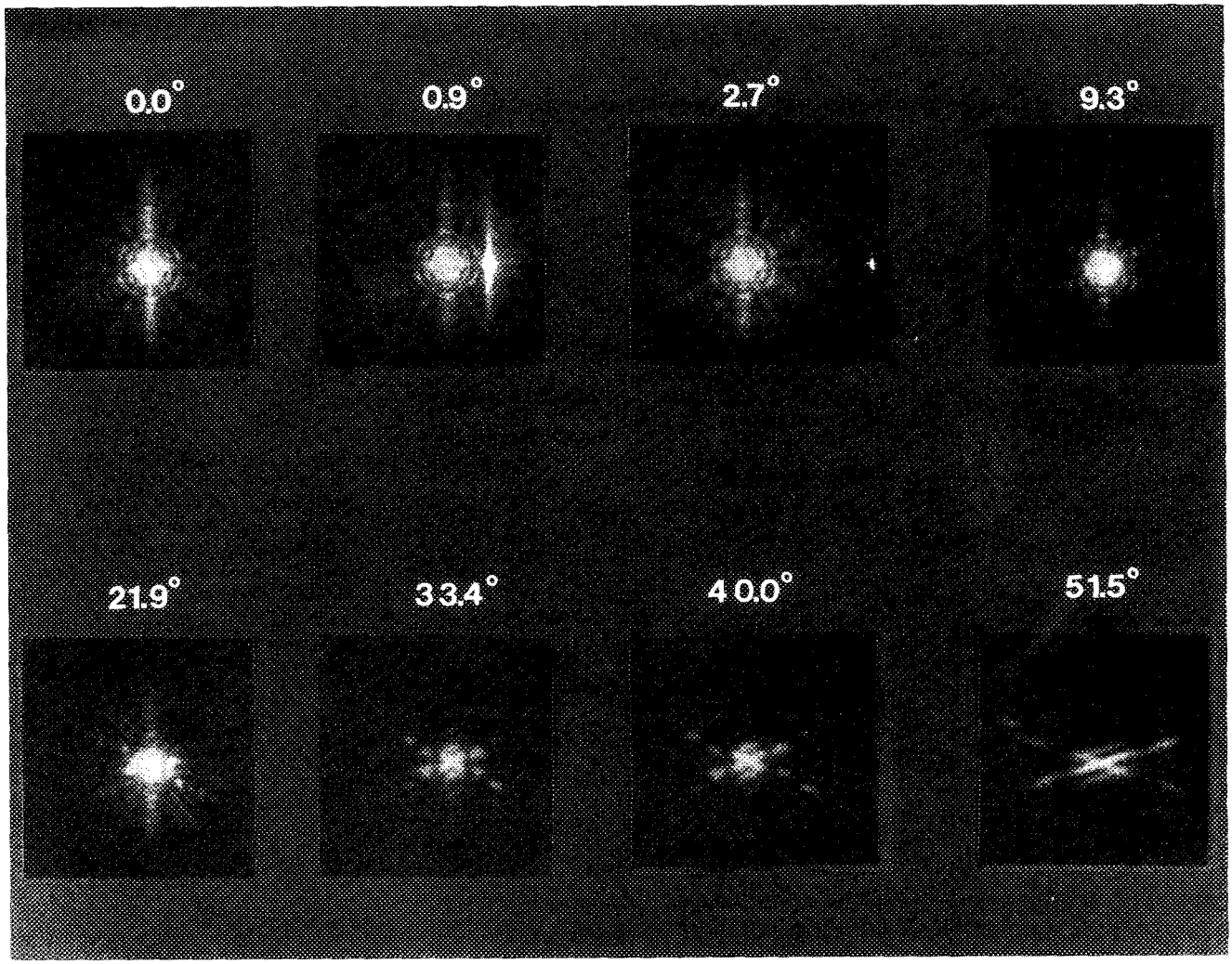

FIG. 3. Diffraction patterns of retroreflected light from He–Ne laser illumination. Angle of incidence as shown in the figure.

the array elements, and the multiple beam interference from light reflected from the individual array elements. The diffraction patterns do not change appreciably up to about 9° incident angle. Above 30° the pattern is severely distorted from its normal incidence appearance.

The 12 spokes in the pattern arise from diffraction from the triangular apertures of individual reflectors. They are composed of two sets of six spokes. In each set the spacing is 60°. The brighter set is from the aperture edges. The fainter set is from the three dihedral edges of the corner cubes. The circular rings in the pattern are due to laser aperture diffraction. The diffraction orders on the spokes are from light retroreflected from the array elements. Other diffraction sources or phase shifts from path length differences may also make relatively minor contributions to the pattern.

The specular reflection components from single-surface reflections are out of the field of view of the camera. At normal incidence these appear as six spots arranged 60° apart along a cone oriented about 67° to the array normal. The bright spot which tracks the angle of incidence is primarily Fresnel reflection from the front surface of the array. Superimposed on this reflection are reflections from edges of the array elements and the zero-order (specular) component of the retroreflection.

The interference effects are examined in more detail in Fig. 4, which shows quantitative measurements along the bright spoke containing the front-surface reflection. The measurements were made with a resolution of about 3 mrad. They demonstrate that at up to relatively large angles of incidence ($\leqslant$0.5 rad) 90% or more of the retroreflected light goes into the first order. A small amount of light appears in the second order, which is centered at $\pm$ 8 mrad.

The observed behavior is in only qualitative agreement with Eq. (1). Equation (1) predicts more sharply defined orders and less light appearing in higher orders than actually observed. The assumption of one-dimensional interference is probably the major source of errors in the predictions. The choice of a rectangular aperture function also contributes to errors.

Figure 5 shows the change of integrated retroreflection intensity as a function of incident angle. The sharp decrease of intensity at low incident angles is due to the movement of the front surface specular reflection out of the detector. After this reflection vanishes from the detector, the retrore-

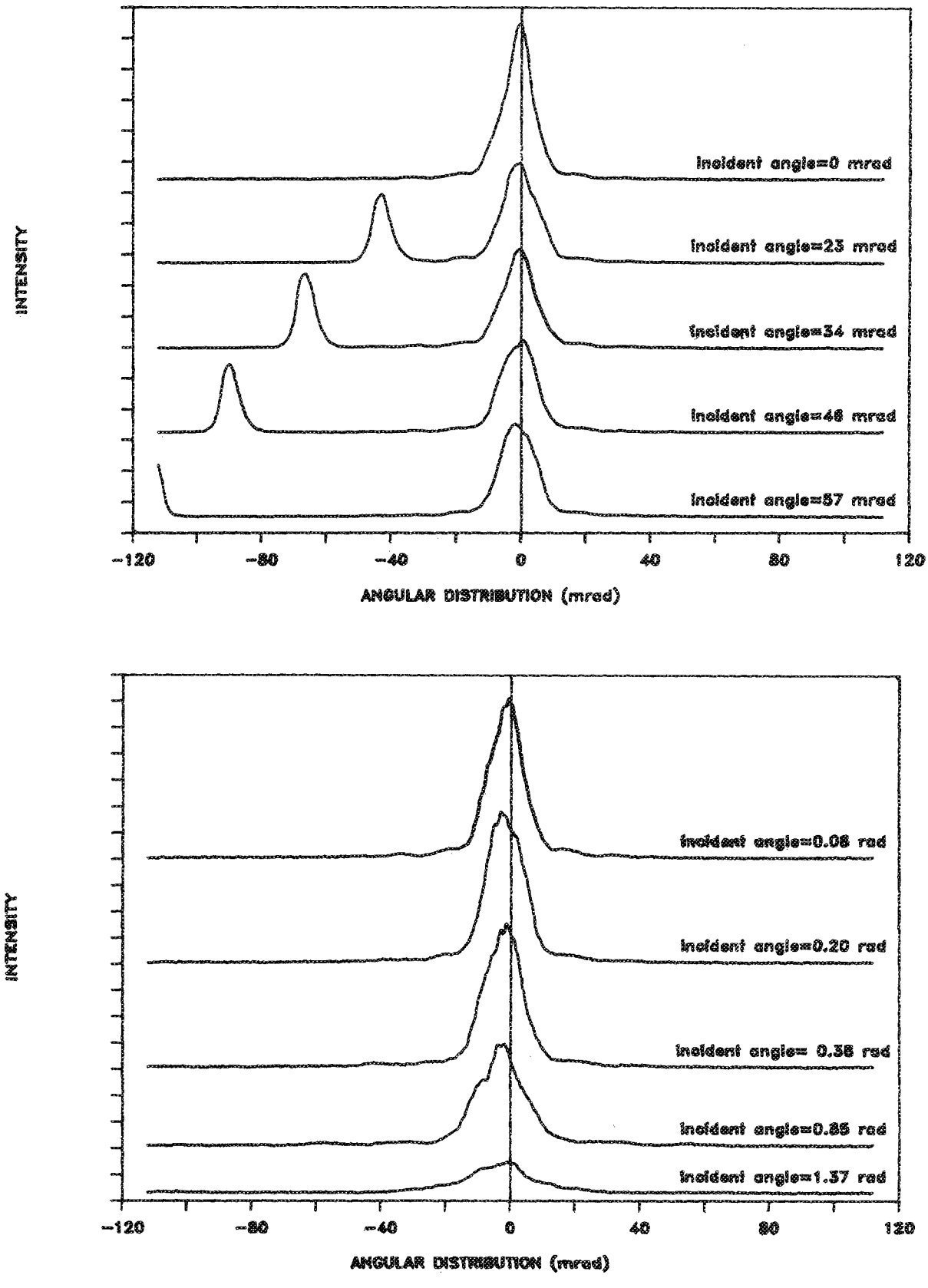

FIG. 4. Diffraction pattern from He–Ne laser illumination of RRA. Angular intensity profiles of retroreflected light at varying angles of incidence, as shown in figure. The specular reflection signal is not shown for angles of incidence 0.08 rad and greater.

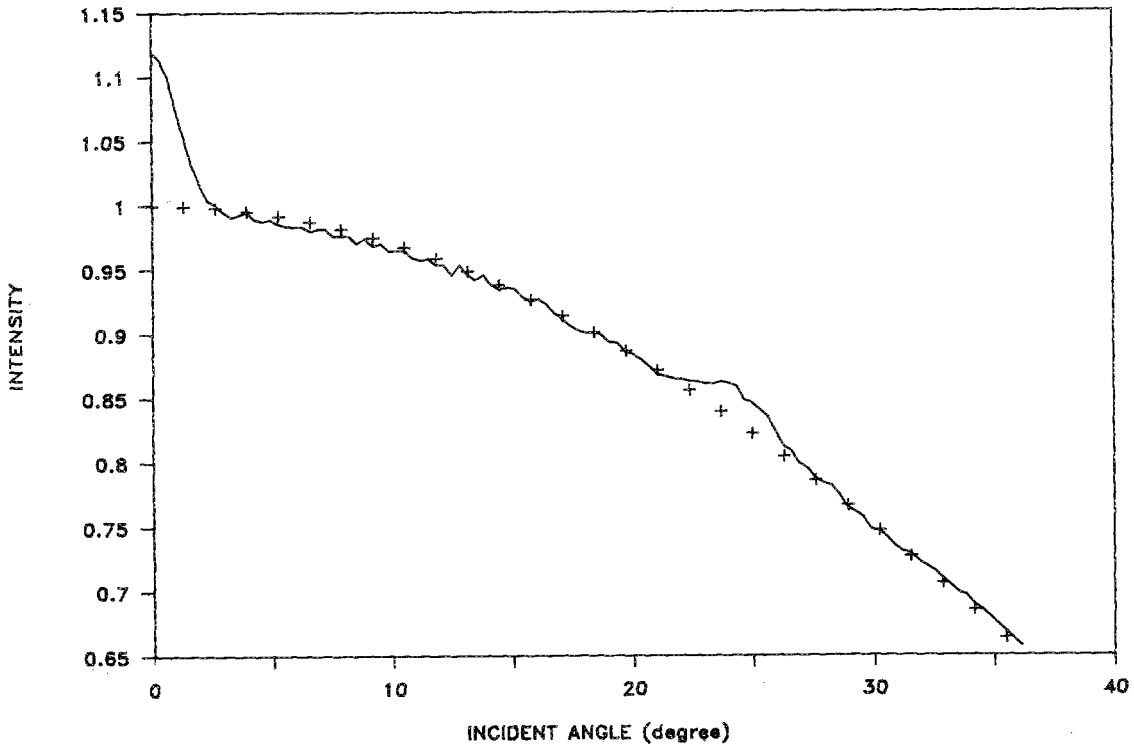

FIG. 5. Integrated retroreflection intensity from collimated He–Ne laser beam of as a function of incident angle. The solid line is experimental data. The crosses are calculated points from a $\cos^2 \theta_i$ fit.

flection intensity decreases with a $\cos^2 \theta_i$ dependence. This dependence follows the change in projected area of the array normal to the direction of illumination. The $\cos^2 \theta_i$ dependence is interrupted at $\theta_i \simeq 23°$. At this angle a component of the single surface reflection is directed back along the retroreflection direction.

Figure 6 demonstrates the finite divergence correction obtainable with the retroreflective array. The return beams from incident beams of 1–40-mrad divergence always have divergences of about 6 mrad ($1/e^2$ intensity, half-angle). This divergence is only somewhat greater than the calculated diffraction limit. Taking the effective aperture to be 0.147 mm, the diffraction-limited divergence is about 4.3 mrad. Although collimation does not affect the divergence, it does

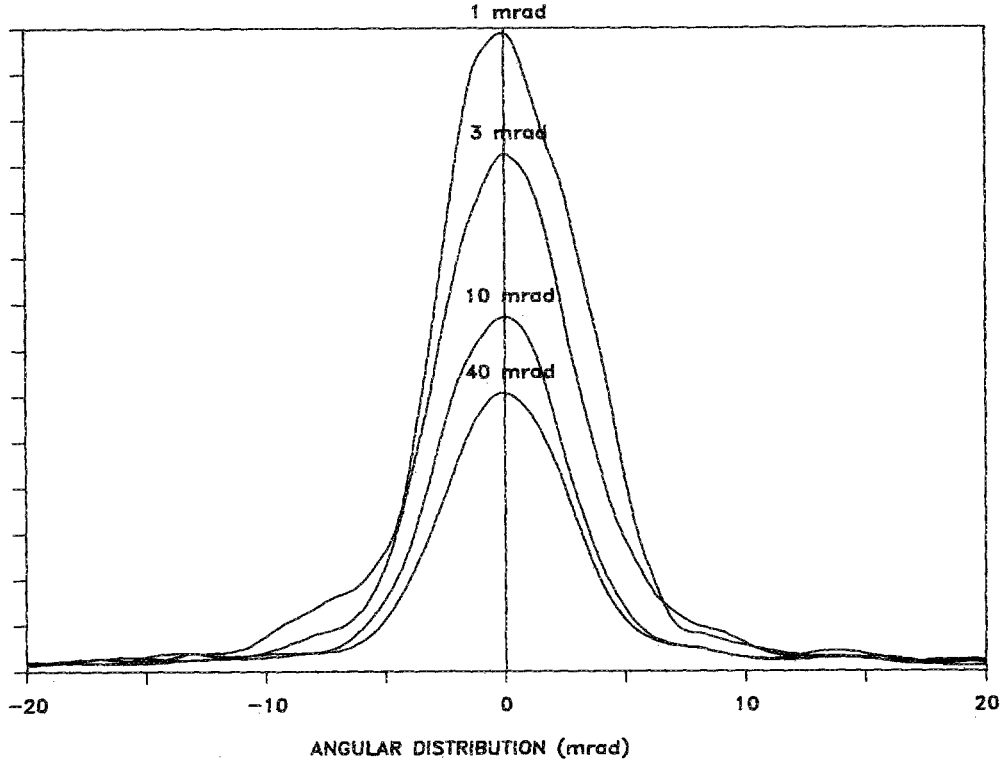

FIG. 6. Angular distribution of retroreflected light from illumination with He–Ne laser beam of divergence 1–40 mrad.

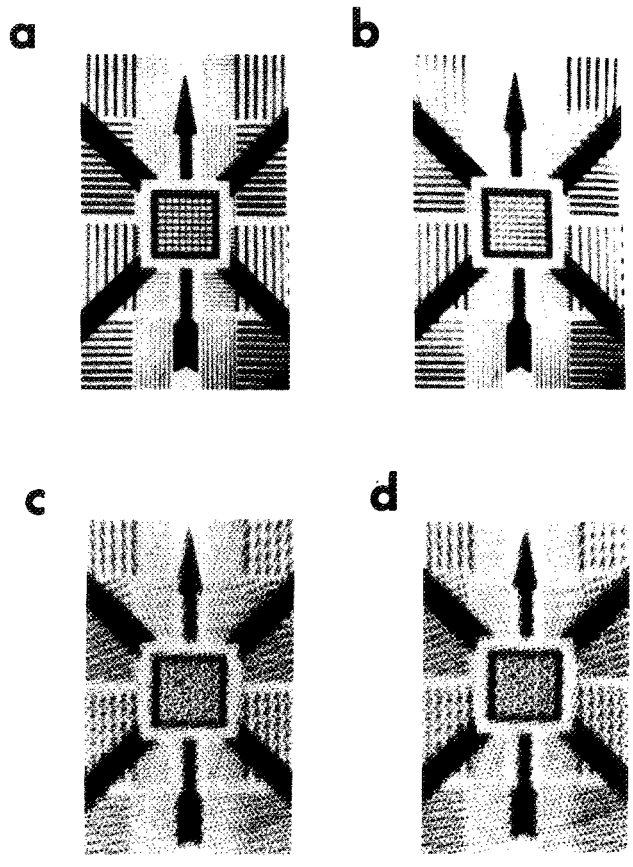

FIG. 7. Comparison of the imaging properties of a plane mirror and a retroreflective array, using apparatus of Fig. 2(b). (a) Plane mirror, no phase perturbation; (b) plane mirror, phase perturbation from heated air; (c) retroreflective array, no phase perturbation; (d) retroreflective array, phase perturbation from heated air. The images are magnified eight times.

affect the efficiency of the array.

Figure 7 shows the results of a test of imaging performance of a plane mirror and a retroreflective array with and without the presence of a phase perturbation. The photographs were made with the apparatus of Fig. 2(b), using coherent illumination. Figure 7(a) shows the image after reflection from a plane mirror without the phase perturbation generated by heating the air in the light path. The resolution is good. All lines appear straight and the center square is undistorted. Figure 7(b) shows the image after reflection from the same mirror, but with the air along the light path perturbed by heat from the hot plate. Because the mirror does no phase correction, the lines are bent, the grid in the center square is distorted, and the central square is distorted to a parallelogram. When viewed, the image appeared to flicker, in response to changing air currents.

In contrast to the plane mirror, the retroreflective array always produces a discontinuous image, as shown in Fig. 7(c), because of the local inversions of the corner cubes. Diffractive and geometric spreading limit the registration of adjacent components. However, when the phase perturbation was introduced, there was no change in the image, as shown in Fig. 7(d). That image is indistinguishable from the image of Fig. 7(c). Visual observation showed no movement in the image in response to changing air currents.

The retroreflective array works well for both coherent and incoherent light source. Images rendered by the coherent light source have better contrast. The incoherent source gives better resolution with this test pattern. This observation may not be general because the effects of coherent and incoherent illumination will depend on the phase distribution of the object illuminated. Nonetheless, we can conclude that retroreflective array corrects phase errors in either type of illumination.

IV. CONCLUSIONS

The RRA in the phase conjugation configuration is potentially useful in any system which is not shot-noise limited. In practice, most absorbance measurements are not made under shot-noise limited conditions if the sample is nonisothermal, is in motion, or consists of imperfectly mixed components. The excess noise is usually sufficiently large that real performance improvements can be expected.

The thermal conductivities of water and most common solvents are about 1×10^{-3} cm^2/s.[12] Heat conduction occurs over a distance of approximately $\sqrt{Dt}$. This distance is about 0.1–0.3 mm for a 0.1–1-s measurement time. In a liquid system, thermally generated refractive index gradients can extend over these distances in liquids. Therefore, for 0.1–1-s measurements, an aperture size somewhat smaller than 0.1 mm is desirable. Larger apertures are tolerable in gas phase systems, since thermal diffusivities are larger and refractive index gradients will extend over larger distances.

The data of Figs. 3 and 4 show that at angles of incidence as high as 30° at least 90% of the retroreflected light appears in the first order, the nominal phase conjugation direction. Only a small percentage appears in the second or higher orders, or in zero-order (specular reflection) interference. Therefore, the phase correction performance of an array is maintained over all practical spectroscopic conditions. However, the presence of small higher-order components and the finite divergence of the return beam mean that a retroreflective array cannot provide perfect correction for phase perturbations. Our data do not provide unambiguous information on the upper limit of the correction.

Light losses from single- and two-surface reflections are inevitable with the RRA. Light losses increase with beam divergence or angle of incidence, as shown in Figs. 5 and 6. In order to maximize the efficiency of the array, it is advisable to illuminate it with light which has been roughly collimated. Collimation to 1°–2° is adequate.

To eliminate potential problems with zero-order (specular) reflection, the array should be slightly tilted with respect to the normal to the incident light beam. Any angle below about 10° which directs the specular component away from the detector will eliminate specular reflection and generate efficiency losses of less than 10%. Because Reflexite is a second-surface reflector front-surface reflections also degrade its performance. This problem would be completely absent from front-surface arrays.

It is clear from Fig. 7 that in the absence of phase perturbations mirrors are better imaging devices than retroreflective arrays. In an analytical absorption measurement, it is the spatially integrated response over the active area of the detector which is usually measured. The image quality is of

no direct concern. The spatial stability of the intensity distribution is important. Detector response imhomogeneities and changes in the intensity of radiation illuminating the monochromator slits or other limiting apertures are sources of excess noise if the image is unstable. In a spectroscopic application, the retroreflective array is clearly the superior choice.

Many absorbance measurements can benefit from the use of a retroreflective array. Surprisingly good results have been obtained with low-quality replica arrays. Arrays with 10–20 elements/mm constructed to diffraction grating standards, and usable in the ultraviolet, should greatly extend the range of application of the phase conjugation optical configuration.

ACKNOWLEDGMENT

This work was supported in part by National Science Foundation grant CHE-8317861.

[1]H. H. Barrett and S. F. Jacobs, Opt. Lett. **4**, 190 (1979).
[2]S. F. Jacobs, Opt. Eng. **21**, 281 (1982).
[3]T. R. O'Meara, Opt. Eng. **21**, 271 (1982).
[4]K. V. K. Orlov, Ya. Z. Virnik, S. P. Vorotilin, V. B. Gerasimov, Yu. A. Kalinin, and A. Ya. Sagalovich, Sov. J. Quantum Electron. **8**, 799 (1978).
[5]P. Mathieu and P. A. Bélanger, Appl. Opt. **19**, 2262 (1980).
[6]Z. E. Bagdasarov, Ya. Z. Virkik, S. P. Vorotilin, V. B. Gerasimov, V. M. Zaika, M. V. Zakharov, V. M. Kazanskiĭ, Yu. A. Kalinin, V. K. Orlov, A. K. Piskunov, A. Ya. Sagalovich, A. F. Suchkov, and N. D. Ustinov, Sov. J. Quantum Electron. **11**, 1465 (1981).
[7]B. K. Barikhin, K. P. Barkosvkiĭ, V. B. Gerasimov, A. L. Dudarevich, E. V. Kudryavkin, V. I. Nedolugov, V. K. Orlov, A. G. Petukhov, V. I. Ral'chenko, and A. I. Chernomordin, Sov. J. Quantum Electron. **15**, 1139 (1985).
[8]T.-K. J. Pang and M. D. Morris, Anal. Chem. **57**, 2700 (1985).
[9]Y.-Z. Hsieh, E. T. Johnson, R. D. Sacks, and M. D. Morris, Appl. Spectrosc. (in press).
[10]B. Ya. Zel'dovich, N. F. Pilipetsky, and V. V. Shkunov, in *Principles of Phase Conjugation* (Springer, Berlin, 1985).
[11]I. M. Bel'dyugin, Sov. J. Quantum Electron. **11**, 1435 (1981).
[12]A. Rosencwaig, in *Photoacoustic and Photoacoustic Spectroscopy* (Wiley-Interscience, New York, 1980).